VIRAL IMMUNITY

Influenza restriction factor MxA functions as inflammasome sensor in the respiratory epithelium

SangJoon Lee[1], Akari Ishitsuka[2], Masayuki Noguchi[3], Mikako Hirohama[1], Yuji Fujiyasu[4], Philipp P. Petric[5,6,7], Martin Schwemmle[5,6], Peter Staeheli[5,6], Kyosuke Nagata[1], Atsushi Kawaguchi[1,2,8,9]*

The respiratory epithelium is exposed to the environment and initiates inflammatory responses to exclude pathogens. Influenza A virus (IAV) infection triggers inflammatory responses in the respiratory mucosa, but the mechanisms of inflammasome activation are poorly understood. We identified MxA as a functional inflammasome sensor in respiratory epithelial cells that recognizes IAV nucleoprotein and triggers the formation of ASC (apoptosis-associated speck-like protein containing a CARD) specks via interaction of its GTPase domain with the PYD domain of ASC. ASC specks were present in bronchiolar epithelial cells of IAV-infected MxA-transgenic mice, which correlated with early IL-1β production and early recruitment of granulocytes in the lungs of infected mice. Collectively, these results demonstrate that MxA contributes to IAV resistance by triggering a rapid inflammatory response in infected respiratory epithelial cells.

INTRODUCTION

Influenza A virus (IAV) causes severe inflammation in the respiratory tract and leads to more than 500,000 annual deaths worldwide. The proinflammatory response triggers migration of immune cells, including macrophages and neutrophils, to remove infectious agents. Among the proinflammatory cytokines, interleukin-1β (IL-1β) is a key mediator of the inflammatory response and is essential for resistance to IAV infection (*1*–*4*). The secretion of IL-1β is controlled through proteolytic maturation of pro–IL-1β mediated by inflammasomes, which are multiprotein complexes consisting of caspase-1, ASC, and cytoplasmic pathogen recognition receptors (PRRs) such as NOD (nucleotide-binding oligomerization domain)–like receptor family proteins (NLRPs) (*5*). PRRs undergo self-oligomerization in response to viral ligand recognition and recruit the pivotal adaptor protein ASC for the formation of inflammasomes. ASC is composed of an N-terminal pyrin domain (PYD) and a C-terminal caspase recruitment domain (CARD). ASC oligomerizes through homotypic interactions of the PYD domain and subsequently recruits caspase-1 via the CARD domain. In macrophages, NLRP3 recognizes IAV infection by sensing the disturbances in intracellular ionic concentrations caused by viral protein M2 (*6*). Because NLRP3 is expressed in macrophages but not in epithelial cells, it has been believed that macrophages are responsible for the inflammatory response during IAV infection. However, emerging lines of evidence have shown that the respiratory epithelium is not only a physical barrier separating the host from the external environment but also a sensor of infectious agents to initiate the proinflammatory response (*7*). We recently demonstrated that IL-1β is secreted through inflammasome activation in IAV-infected normal or precancerous human bronchial epithelial cells under the control of type I interferon (IFN) signaling (*8*). This finding implies the existence of an unknown mechanism that activates the inflammasomes in human respiratory epithelial cells against IAV infection.

Here, we identified human myxovirus resistance protein 1 (MxA) as an inflammasome sensor molecule in human respiratory epithelial cells upon IAV infection. Expression of *Mx* genes is controlled by type I and III IFNs. Mx proteins are evolutionarily conserved dynamin-like large guanosine triphosphatases (GTPases) and are potent antiviral factors restricting a variety of viruses including IAV (*9*, *10*). MxA forms dimers and tetramers in a criss-cross fashion and further oligomerizes into ring-like structures at a higher protein concentration (*11*, *12*). Although the detailed mechanism of Mx-mediated antiviral activity remains unknown, MxA targets viral ribonucleoprotein (RNP) complexes of RNA viruses (*10*). The interaction of Mx protomers with viral RNPs is believed to recruit additional Mx molecules to form higher-order oligomeric rings on viral RNPs (*13*, *14*). This suggests that MxA may entrap incoming viral RNPs to inhibit the nuclear import of viral RNPs and subsequent viral RNA synthesis (*15*–*18*). Oligomerization facilitates the GTPase activity of MxA, which drives the mechanical constriction of the MxA ring, possibly leading to the disruption of viral RNPs (*19*). Avian IAV strains are more strongly restricted by MxA than human isolates (*20*–*25*). A cluster of escape mutations from MxA restriction was identified in the body domain of nucleoprotein (NP). Such mutations are believed to facilitate the transmission of avian IAVs from their natural reservoir (wild aquatic birds) to humans (*24*).

By high-content short hairpin RNA (shRNA) library screening, we identified MxA as a cellular factor that is required for inflammasome formation in response to IAV infection in human respiratory epithelial cells but not in macrophages. MxA directly interacted with ASC and stimulated the assembly of ASC oligomers in infected respiratory epithelial cells. Further, IL-1β secretion was rapidly induced in the respiratory epithelium of IAV-infected MxA-transgenic (hMx-Tg) mice in an NLRP3-independent manner, and the rapid inflammatory response protected the animals from IAV infection by repressing virus spread from the bronchioles to distal alveolar regions. It is also suggested that the MxA inflammasome helps restricting the zoonotic transmission of avian IAV strains to humans by recognizing the NP

[1]Department of Infection Biology, Faculty of Medicine, University of Tsukuba, Tsukuba, Japan. [2]PhD Program in Human Biology, School of Integrative and Global Majors, University of Tsukuba, Tsukuba, Japan. [3]Department of Pathology, Faculty of Medicine, University of Tsukuba, Tsukuba, Japan. [4]School of Medicine, University of Tsukuba, Tsukuba, Japan. [5]Institute of Virology, University Medical Center Freiburg, Freiburg, Germany. [6]Faculty of Medicine, University of Freiburg, Freiburg, Germany. [7]Spemann Graduate School of Biology and Medicine, University of Freiburg, Freiburg, Germany. [8]Transborder Medical Research Center, University of Tsukuba, Tsukuba, Japan. [9]Microbiology Research Center for Sustainability, University of Tsukuba, Tsukuba, Japan.
*Corresponding author. Email: ats-kawaguchi@md.tsukuba.ac.jp

protein from avian IAV strains. Collectively, we propose that MxA functions as an inflammasome sensor against IAV infection in respiratory epithelial cells and that this rapid MxA-triggered inflammatory response contributes to IAV resistance.

RESULTS

Identification of MxA as an inflammasome sensor in human respiratory epithelial cells upon IAV infection

To identify a respiratory epithelium-specific inflammasome sensor, we performed a high-content shRNA library screen with immortalized human atypical adenomatous hyperplasia (PL16T) cells to identify a putative respiratory epithelium–specific inflammasome sensor (fig. S1, A and B). This screen showed that *CTSL1*, *MOGS*, *PTPN7*, *SERTAD2*, and *MxA* genes influenced inflammasome formation in infected PL16T cells, of which *MxA* had the most pronounced effect (Fig. 1A). Knockdown (KD) of these genes did not impair ASC speck formation in IAV-infected THP-1 macrophages (Fig. 1B). The amount of these mRNAs in shRNA-treated cells decreased to less than 5% of that in control cells (fig. S2, A to E). Viral NP levels were not reduced in these shRNA-treated cells compared with control cells, suggesting that virus infectivity was not impaired by KD of these genes (fig. S3, A and B). Interaction between MxA and endogenous ASC was observed by immunoprecipitation using anti-ASC antibody (Fig. 1C). We next performed time-resolved fluorescence energy transfer (TR-FRET) assays with recombinant His-MxA and biotinylated MBP-ASC proteins (fig. S4). MxA is a dynamin-like large GTPase and composed of an N-terminal GTPase domain and a stalk domain consisting of a central middle domain (MD) and a C-terminal GTPase effector domain (GED) (*10*). ASC interacted with wild-type MxA (residues 1 to 662) and the GTPase domain [residues 38 to 366-$(GS)_5$–622 to 662] of MxA but not the stalk domain (residues 367 to 621) (Fig. 1D). We also found that the MxA-GTPase domain interacts with the ASC-PYD domain more than the

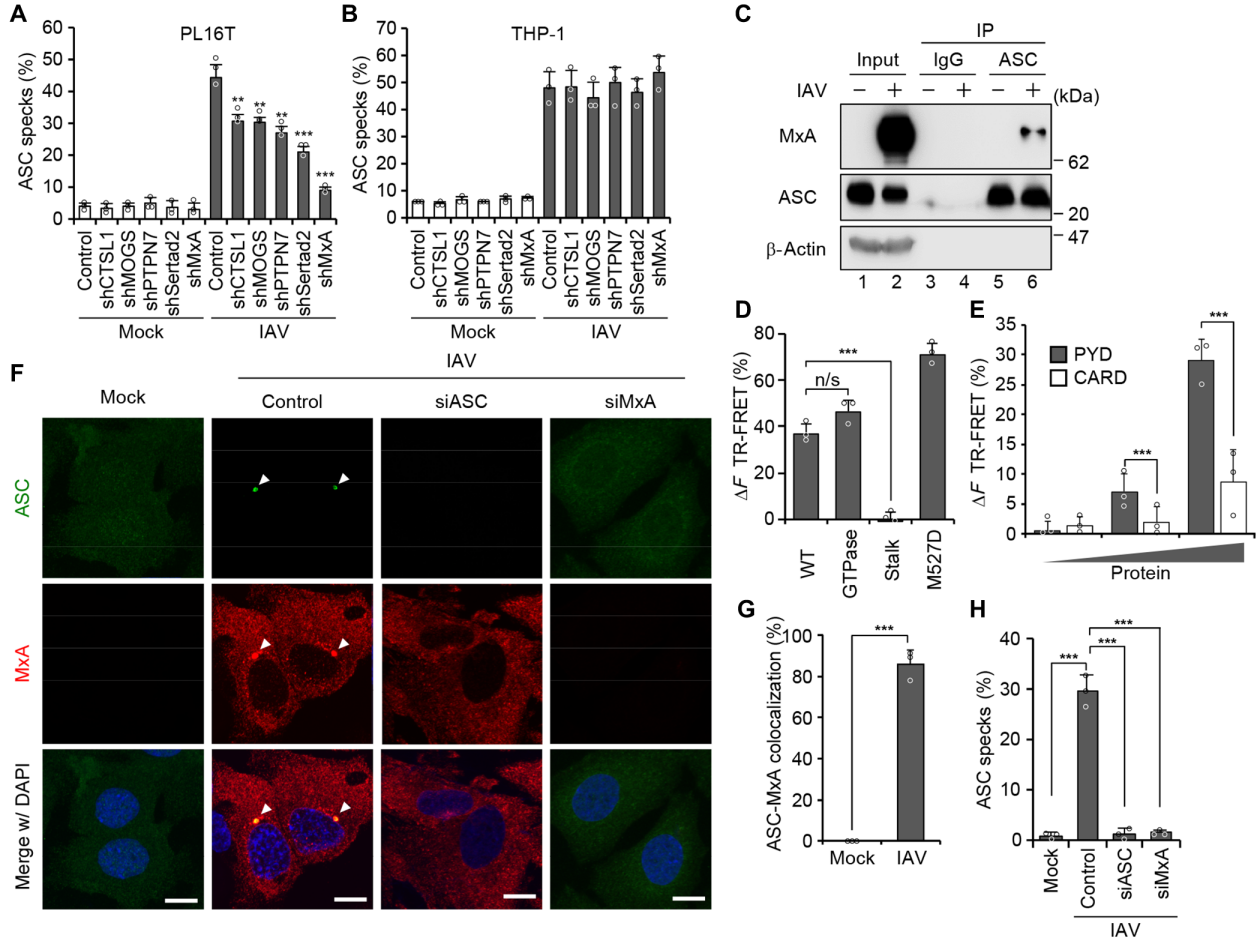

Fig. 1. Identification of MxA as an inflammasome sensor in human respiratory epithelial cells upon IAV infection. (**A** and **B**) ASC speck formation at 36 hours after infection in FLAG-GFP-ASC PL16T cells (A) and FLAG-GFP-ASC THP-1 cells (B) treated with the indicated shRNA lentiviruses (means ± SD from three independent experiments). (**C**) At 48 hours after infection, infected PL16T cells were subjected to immunoprecipitation (IP) with either nonspecific IgG or anti-ASC antibodies. (**D**) TR-FRET signal between MBP-ASC wild-type (WT) (10 nM) and MxA variants (10 nM) including His-MxA wild-type, His-MxA-GTPase, His-MxA-stalk, and His-MxA M527D was examined (means ± SD from three independent experiments). (**E**) TR-FRET signal between His-MxA-GTPase (10 nM) and increasing concentration of MBP-ASC-PYD or MBP-ASC-CARD (0.4, 2, and 10 nM) was examined (means ± SD from three independent experiments). (**F** to **H**) PL16T cells treated with siControl, siASC, or siMxA were subjected to indirect immunofluorescence assays with anti-ASC (green) and anti-MxA (red) antibodies at 48 hours after infection (F). Arrowheads indicate ASC specks. Scale bars, 5 μm. The number of cells showing accumulating pattern of MxA in ASC specks was counted ($n > 100$) (G). The number of ASC specks was counted ($n > 100$) (H). $^{**}P < 0.01$ and $^{***}P < 0.001$, two-tailed Student's *t* test. Data are representative of three independent experiments (C and F). DAPI, 4′,6-diamidino-2-phenylindole.

ASC-CARD domain (Fig. 1E). This suggests that MxA directly interacts with ASC through interaction of the MxA-GTPase domain mainly with the ASC-PYD domain. ASC also interacted with an MxA monomeric mutant (M527D; Fig. 1D) (*13*), suggesting that this interaction did not result from nonspecific binding owing to entanglement of MxA and ASC oligomers. Further, MxA colocalized with ASC specks in about 30% of infected PL16T cells at 36 hours after infection in an ASC-dependent manner (Fig. 1, F to H). This is in agreement with a previous finding that the inflammasome is activated in a fraction of infected cells that overcame apoptosis, possibly by anti-apoptotic function of NS1 viral protein (*8*).

To elucidate whether MxA is required for inflammasome activation in respiratory epithelial cells, we examined IL-1β secretion from MxA KD cells. IL-1β secretion from infected human peripheral blood mononuclear cell (PBMC)–derived macrophages was dependent on NLRP3 but not on MxA (Fig. 2A). In contrast, MxA KD reduced the amount of secreted IL-1β to about 20% of that secreted from PL16T (Fig. 2B) and primary normal human bronchial epithelial (NHBE) cells (Fig. 2C) transfected with scrambled small interfering RNA (siRNA). Similar results were obtained for IL-18 secretion in infected PL16T cells and THP-1 macrophages (fig. S5, A and B). Further, we found that the amount of secreted IL-1β from infected PL16T cells was not reduced by either siAIM2 (absent in melanoma 2) or siNLRC4 (NLR family CARD domain-containing protein 4) treatment (fig. S6A). The KD of MxA reduced the proteolytic activation of IL-1β in PL16T cells but did not impair the induced expression of pro–IL-1β (fig. S6B). Expression of NLRP3, MxA, AIM2, NLRC4, and ASC was silenced by siRNA treatment without affecting virus infectivity (fig. S6, C to I).

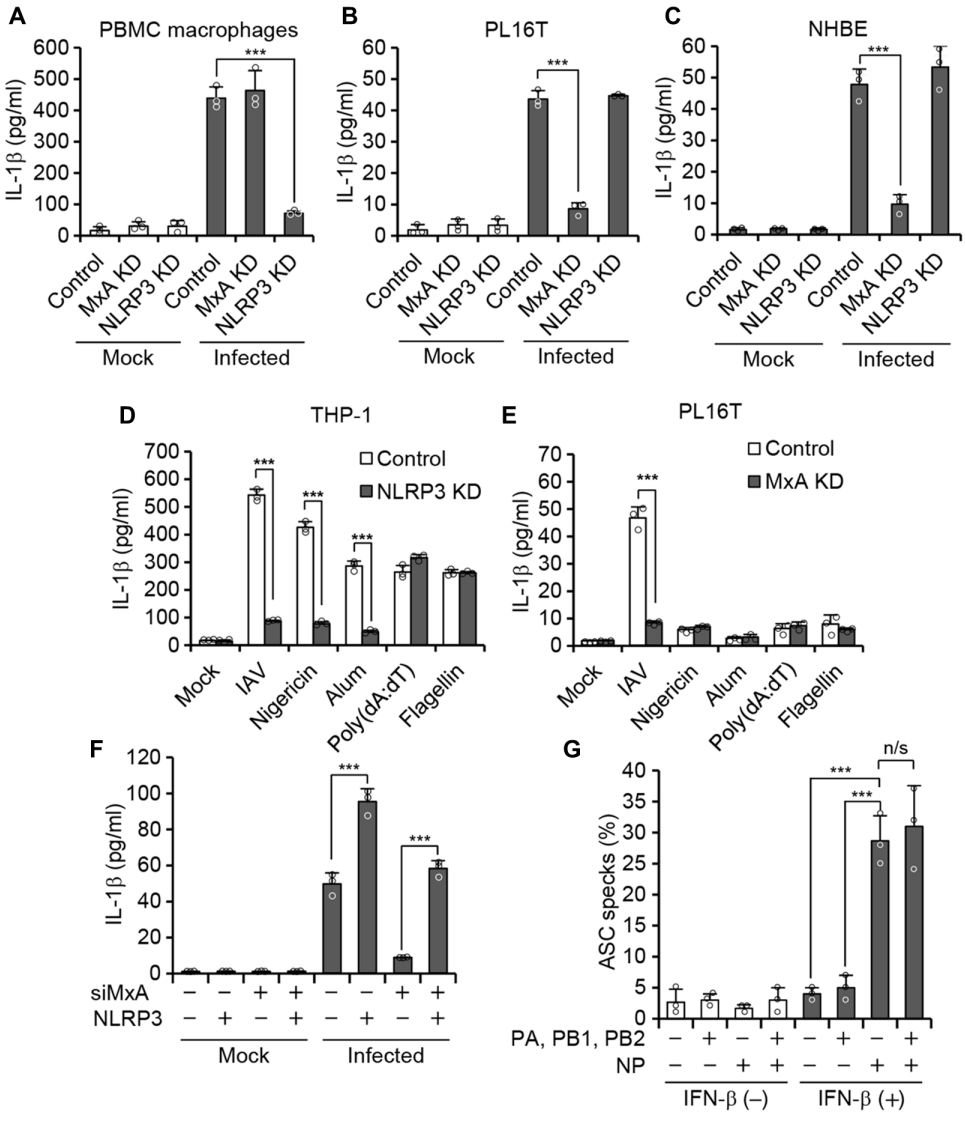

Fig. 2. MxA triggers IL-1β secretion in respiratory epithelial cells upon IAV infection. (**A** to **C**) Level of secreted IL-1β from PBMC macrophages (A), PL16T cells (B), and NHBE cells (C) treated with siControl, siMxA, or siNLRP3 was examined by enzyme-linked immunosorbent assay (ELISA) at 72 hours after infection (means ± SD from three independent experiments). (**D** and **E**) At 48 hours after transfection of the indicated siRNAs, the level of secreted IL-1β from THP-1 macrophages (D) and PL16T cells (E) was examined by ELISA after treatment with IAV, nigericin (5 μg/ml), alum (250 μg/ml), poly(dA:dT) (3 μg/ml), or flagellin (500 ng/ml) at 72 hours after treatment (means ± SD from three independent experiments). (**F**) The level of secreted IL-1β from MxA KD PL16T cells expressing NLRP3 was examined by ELISA at 72 hours after infection (means ± SD from three independent experiments). (**G**) PL16T cells were transfected with plasmids expressing PA, PB1, PB2, or NP from PR8 strain. After incubating with IFN-β (1000 IU/ml) for 36 hours, ASC specks were counted (means ± SD from three independent experiments). ***$P < 0.001$, two-tailed Student's *t* test.

We next examined various stimuli that are recognized by other inflammasome sensors, such as nigericin and alum for NLRP3 (*26*), poly(dA:dT) [poly(deoxyadenylic-deoxythymidylic)] for AIM2 (*27*), and flagellin for NLRC4 (*28*). As previously reported, IL-1β was secreted from THP-1 macrophages upon stimulation by IAV infection, nigericin, and alum in an NLRP3-dependent manner (Fig. 2D). In contrast, IL-1β was secreted from PL16T cells after IAV infection but not after treatment with other stimuli (Fig. 2E). We tested whether MxA KD can be rescued by exogenous expression of NLRP3 in PL16T cells. NLRP3 is expressed in macrophages (*29*) but not in epithelial cells (fig. S7). The reduction of IL-1β secretion by MxA KD was complemented by NLRP3 expression in PL16T cells (Fig. 2F and fig. S8). MxA interacts with viral RNP complexes consisting of viral polymerases and NP (*30*). To determine which viral component(s) are recognized as a ligand by the MxA inflammasome, PL16T cells were transfected with viral polymerase subunits and NP from IAV strain PR8 (H1N1) and then treated with IFN-β at 24 hours after transfection to induce expression of endogenous MxA. ASC specks were observed in cells transfected with NP but not the viral polymerase (Fig. 2G and fig. S9). These findings strongly suggest that MxA functions as a sensor of IAV infection in respiratory epithelial cells.

Oligomerization of MxA is required for inflammasome formation

Upon inflammasome activation, ASC assembles into a Triton X-100–insoluble homo-oligomer (*31*), and this oligomerized ASC is required for caspase-1 activation. To analyze the extent of ASC oligomerization, Triton X-100–treated PL16T (Fig. 3) or NHBE (fig. S10) cells were cross-linked with 2 mM bis(sulfosuccinimidyl) suberate and analyzed by Western blotting with anti-ASC antibody. Most of the ASC proteins in the Triton X-100–insoluble fraction were highly oligomerized in infected control cells but not in infected MxA KD cells (Fig. 3A and fig. S10A). In agreement with this, proteolytic activation of caspase-1 was not observed in infected MxA KD cells (Fig. 3B and fig. S10B).

MxA assembles into homo-oligomers through the interaction between MD and GED, and the oligomerization facilitates the GTPase activity of MxA (*11*, *13*, *14*, *32*). MxA is also known to associate with endoplasmic reticulum–Golgi intermediate compartments through the L4 loop (amino acid positions 533 to 561) (*14*). To address the molecular mechanism of inflammasome activation by MxA, we examined ASC oligomerization (Fig. 3C), ASC speck formation (Fig. 3D), and IL-1β secretion (Fig. 3E) in MxA KD PL16T cells expressing siRNA-resistant MxA mutants. The following mutants were analyzed: guanosine triphosphate binding–deficient mutant T103A (*33*); membrane binding–deficient L4 loop mutants K554E, K555E, K556E, and K557E (*34*); monomeric mutant M527D (*13*); and dimeric mutant L617D (*13*). Expression of siRNA-resistant wild-type MxA restored inflammasome formation in infected MxA KD cells (Fig. 3C, lane 4; Fig. 3D, lane 4; and Fig. 3E, lane 4). In contrast, ASC speck formation was only partially restored by expression of mutant T103A or L4 (Fig. 3D, lanes 5 and 6), suggesting that GTPase activity and the membrane-binding activity of MxA are both required for inflammasome formation. Expression of monomeric and dimeric MxA mutants resulted in monomeric and dimeric ASC in the Triton X-100–insoluble fraction, respectively, but was unable to induce highly oligomerized ASC (Fig. 3C, lanes 7 and 8). This strongly suggests that ASC assembles into homo-oligomers dependent on the extent of MxA oligomerization.

Mx genes are evolutionarily conserved and determine host resistance to viral infections (*19*, *35*). The subcellular localization of Mx proteins determines their antiviral specificity (*36*). For example, nuclear Mx proteins (e.g., mouse Mx1) inhibit the growth of viruses that replicate in the cell nucleus (*37*–*39*), whereas human MxA protein is localized in the cytoplasm and exhibits a broad antiviral spectrum (*15*, *40*, *41*). The expression of nuclear mouse Mx1 and cytoplasmic mouse Mx2, which is a paralog of human MxA but is ineffective against influenza virus infection (*10*), did not complement reduced IL-1β secretion in infected MxA KD PL16T cells (Fig. 4, A and B). We next examined the formation of ASC specks in human and porcine primary bronchial epithelial cells upon IAV infection. Porcine Mx1 is localized in the cytoplasm (*42*). ASC specks were observed in infected human and porcine epithelial cells (Fig. 4, C and D), suggesting that inflammasome formation in respiratory epithelial cells against IAV infection is a unique property of cytoplasmic Mx1/MxA proteins.

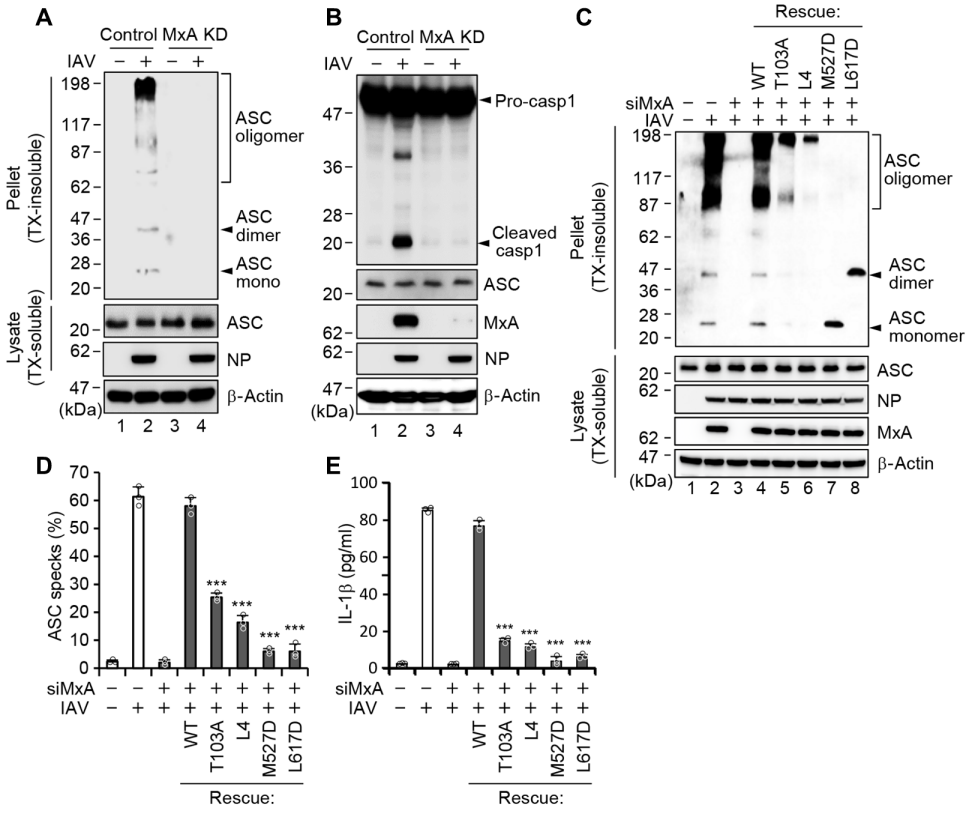

Fig. 3. Oligomerization of MxA is required for inflammasome formation. (**A** and **B**) At 48 hours after infection, oligomerized ASC (A) and cleaved caspase-1 (B) in MxA KD PL16T cells were examined. TX, Triton X-100. (**C** to **E**) At 6 hours after infection with IAV, siRNA-resistant wild-type and indicated MxA mutants were expressed in MxA KD PL16T cells by adding cumate. At 48 hours after infection, ASC oligomerization (C), ASC speck formation (D), and IL-1β secretion (E) were examined (means ± SD from three independent experiments). ***$P < 0.001$, two-tailed Student's *t* test. Data are representative of three independent experiments (A to C).

MxA can also inhibit early steps of viral replication in an ASC-independent manner

Human MxA can trap viral RNPs in the cytoplasm to prevent subsequent steps of viral replication in the nucleus (*10*, *15*–*17*). When we examined the expression level of viral NP in infected PL16T cells at multiplicity of infection (MOI) of 0.1 (Fig. 5A) or 10 (Fig. 5B), a reduction in NP protein levels was observed in infected cells only at MOI of 0.1 in an MxA-dependent manner (Fig. 5A). Every cell in the culture was presumably infected at MOI of 10; however, multiple cycles of infection might proceed at MOI of 0.1. Thus, it is possible that induced expression of MxA by type I and III IFNs in uninfected cells before the spread of progeny viruses is required for MxA-mediated direct inhibition of early steps of viral replication. To address this, we expressed MxA in PL16T cells 12 hours before or 6 hours after IAV infection at MOI of 10 (Fig. 5C). Although the amount of NP was not changed by MxA

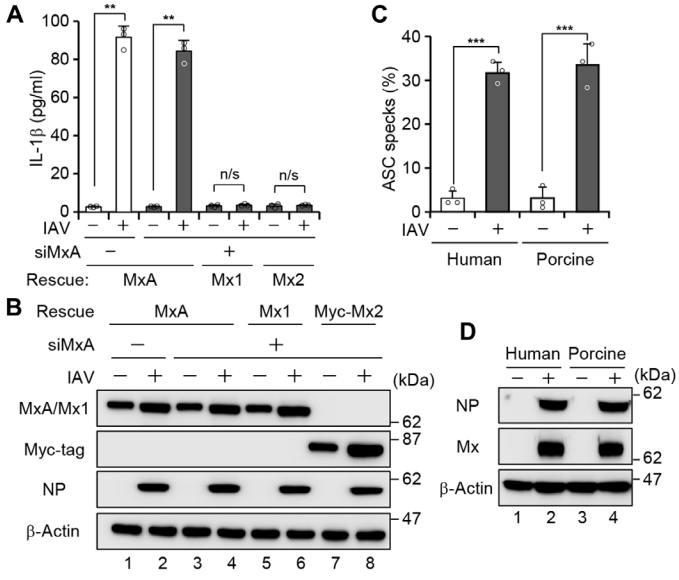

Fig. 4. Cytoplasmic human and porcine Mx1/MxA proteins trigger the inflammasome formation in infected respiratory epithelial cells, whereas nuclear murine Mx1 does not. (**A** and **B**) At 6 hours after infection with IAV, siRNA-resistant MxA, mouse Mx1, or mouse Mx2 was expressed in MxA KD PL16T cells by adding cumate. At 48 hours after infection, IL-1β secretion by ELISA (means ± SD from three independent experiments) (A) and the expression level of NP and Mx proteins (B) were examined. (**C** and **D**) At 48 hours after infection, the number of ASC specks (C) and the expression of NP and Mx (D) in NHBE and porcine bronchial epithelial cells were examined (means ± SD from three independent experiments). $^{**}P < 0.01$ and $^{***}P < 0.001$, two-tailed Student's *t* test. Data are representative of three independent experiments (B and D).

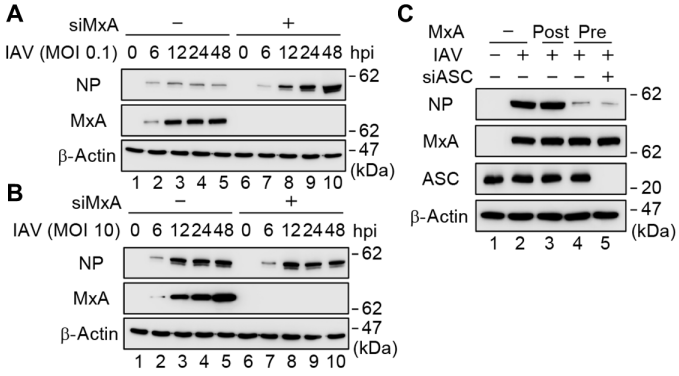

Fig. 5. MxA directly inhibits early steps of the IAV replication cycle in an ASC-independent manner. (**A** and **B**) PL16T cells treated with siControl or siMxA were infected with IAV at either MOI of 0.1 (A) or 10 (B). (**C**) MxA was expressed in PL16T cells by adding cumate after (lane 3) or before IAV infection (lanes 4 and 5) without (lanes 1 to 4) or with siASC treatment (lane 5). The cell lysates were analyzed by SDS-PAGE, followed by Western blot assays with indicated antibodies. Data are representative of three independent experiments (A to C).

expression after infection (Fig. 5C, compare lanes 2 and 3), it was reduced by MxA expression before infection in an ASC-independent manner (compare lanes 2, 4, and 5). Thus, as reported earlier (*10*, *15*), MxA can also restrict IAV infection by inhibiting some early viral replication steps via an inflammasome-independent mechanism.

MxA inflammasome protects mice from IAV infection in respiratory epithelium

Most inbred mouse strains carry defective *Mx* genes due to deletions or a nonsense mutation (*43*). To examine the in vivo function of the MxA inflammasome in a small animal model, we used a transgenic mouse line carrying the entire human *Mx* locus (hMx-Tg) (*21*). In this mouse line, MxA is induced by endogenous type I and III IFNs. As expected, IAV-infected hMx-Tg mice did not lose much body weight (Fig. 6A) and showed better survival compared with nontransgenic (non-Tg) mice (Fig. 6B). We also infected hMx-Tg mice with *Salmonella typhimurium*, which triggers flagellin-dependent NLRC4 inflammasome activation in intestinal epithelial cells (*44*). The susceptibility of hMx-Tg mice against *S. typhimurium* infection was comparable with that of non-Tg mice (Fig. 6C). Thus, MxA does not seem to affect NLRC4-dependent inflammatory responses. At day 3 after IAV infection, the amount of IL-1β in the bronchoalveolar lavage fluid (BALF) obtained from hMx-Tg mice was increased by about threefold in a *Casp1/11*-dependent manner compared with that obtained from non-Tg mice (Fig. 6D). Histological analysis of lung slices of non-Tg mice did not show obvious pathogenic changes at day 3 after IAV infection but showed severe bronchiolitis reducing the alveolar air space, leukocyte infiltration, and desquamation of the bronchiolar epithelium at day 5 after infection (Fig. 6E, top). In contrast, in hMx-Tg mice, a massive infiltration with neutrophils and mononuclear inflammatory cells was observed in the bronchiolar regions at day 3 after infection (Fig. 6E, bottom), and the extent of bronchiolitis was markedly reduced compared with non-Tg mice at day 5 after infection. To quantify the extent of leukocyte infiltration, we further determined the number of leukocytes in the BALF by fluorescence-activated cell sorting (FACS) analysis using anti–Gr-1 antibody as a granulocyte marker. As expected, the number of infiltrating leukocytes in hMx-Tg mice peaked at day 3 after IAV infection but that of non-Tg mice did so only at day 7 after infection (Fig. 6F). Further, the pulmonary viral titer was substantially repressed in hMx-Tg mice in a *Casp1/11*-dependent manner compared with non-Tg mice (Fig. 6G). Thus, it is quite likely that rapid activation of the MxA inflammasome represses virus spread from the bronchioles to the distal alveolar regions. MxA also protected *Casp1/11*$^{-/-}$ mice from low-dose IAV infection (Fig. 6H), suggesting that the MxA-mediated direct inhibition of viral replication is partially responsible for the suppression of IAV infection in vivo.

We next performed immunohistochemical staining of ASC in the infected lung sections. ASC specks were observed in the bronchiolar epithelial cells of hMx-Tg mice but not of non-Tg mice at day 3 after infection [Fig. 7, A and B (arrowheads)]. ASC specks were also colocalized with MxA in the bronchiolar epithelial cells of hMx-Tg mice at day 3 after infection [Fig. 7, C and D (arrowheads)].

Because NLRP3 is responsible for the inflammasome activation in macrophages upon IAV infection, *Nlrp3*$^{-/-}$ non-Tg mice were more susceptible to IAV infection compared with non-Tg mice (Fig. 7E) as previously reported (*3*, *4*). In contrast, hMx-Tg and *Nlrp3*$^{-/-}$hMx-Tg mice survived IAV infection (Fig. 7E). We additionally carried out bone marrow transplantation from *Nlrp3*$^{-/-}$ mice to hMx-Tg recipient mice to exclude the inflammasome response in immune cells (Fig. 7F and fig. S11). The infected non-Tg recipient mice transplanted with *Nlrp3*$^{-/-}$ bone marrow cells did not secrete IL-1β in BALF, suggesting that IL-1β was secreted only from immune cells in an NLRP3-dependent manner. In contrast, IL-1β secretion was still observed in hMx-Tg mice transplanted with *Nlrp3*$^{-/-}$ bone marrow cells (Fig. 7F).

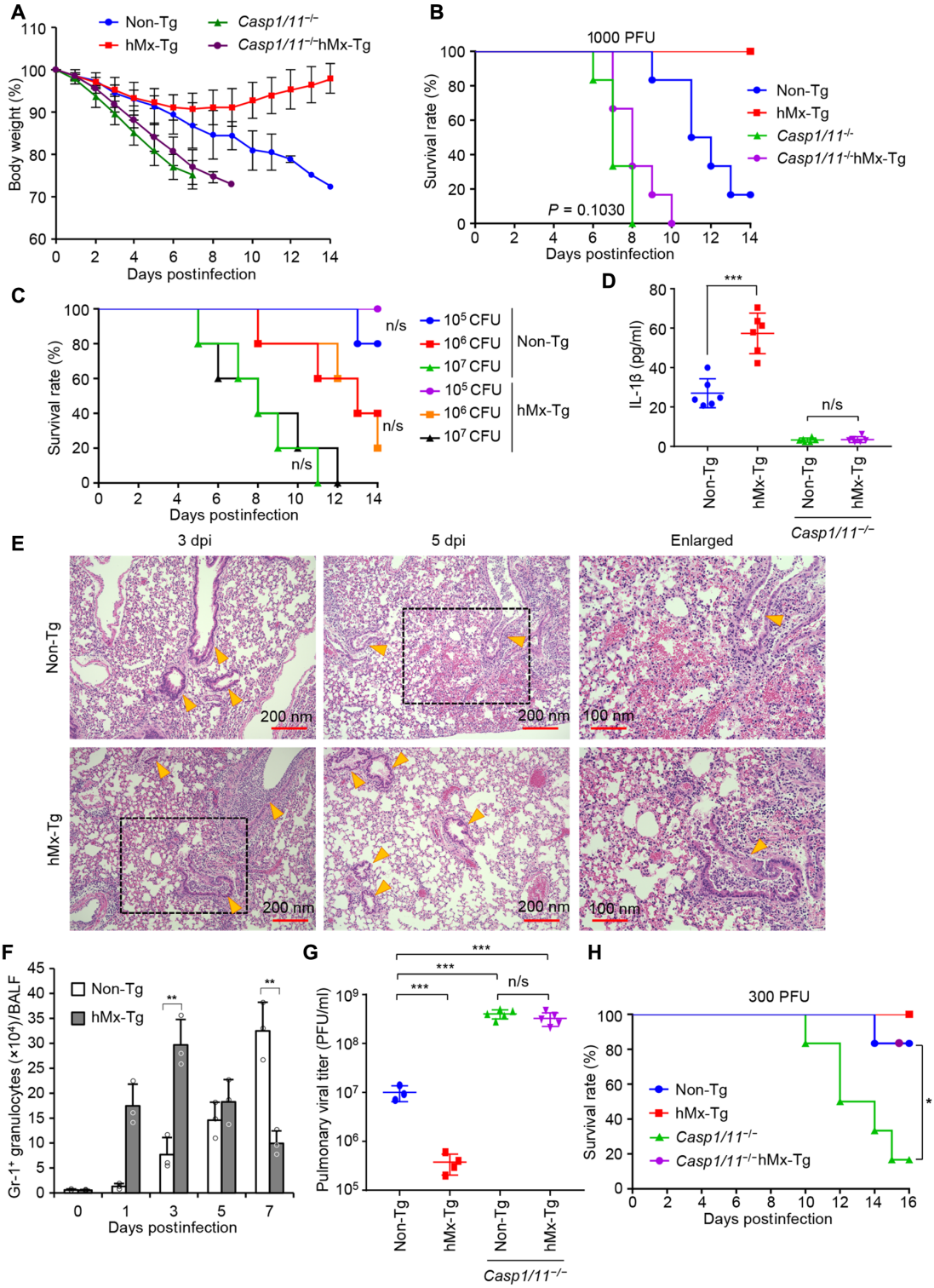

Fig. 6. MxA inflammasome rapidly induces inflammatory response in bronchioles of transgenic mice upon IAV infection. (**A** and **B**) Body weight (A) and survival rate (B) of non-Tg, *Casp1/11*$^{-/-}$, hMx-Tg, and *Casp1/11*$^{-/-}$hMx-Tg mice infected with 1000 PFU of IAV (means ± SD from two independent experiments, $n = 6$ mice per group). $P = 0.1030$ (*Casp1/11*$^{-/-}$ versus *Casp1/11*$^{-/-}$hMx-Tg). (**C**) Non-Tg and hMx-Tg mice were infected with 10^5, 10^6, or 10^7 CFU of *S. typhimurium* ($n = 5$ mice per group). (**D**) The amount of IL-1β in BALF of the indicated mice was examined by ELISA at day 3 after infection ($n = 6$ mice per group). (**E**) Lung tissue sections were stained with hematoxylin and eosin. Arrowheads indicate bronchioles. Data are representative of three independent experiments. dpi, days postinfection. (**F**) Number of Gr-1$^+$ granulocytes in BALF of indicated mice. $^{**}P < 0.01$, two-tailed Student's *t* test. (**G**) Pulmonary viral titer at day 5 after infection ($n = 3$ to 5 mice per group). Each symbol represents one mouse. $^{***}P < 0.001$, two-tailed Student's *t* test. (**H**) Survival rate of non-Tg, *Casp1/11*$^{-/-}$, hMx-Tg, and *Casp1/11*$^{-/-}$hMx-Tg mice infected with 300 PFU of IAV. $^{*}P < 0.05$ (*Casp1/11*$^{-/-}$ versus *Casp1/11*$^{-/-}$hMx-Tg), log-rank test (Mantel-Cox), $n = 6$ mice per group.

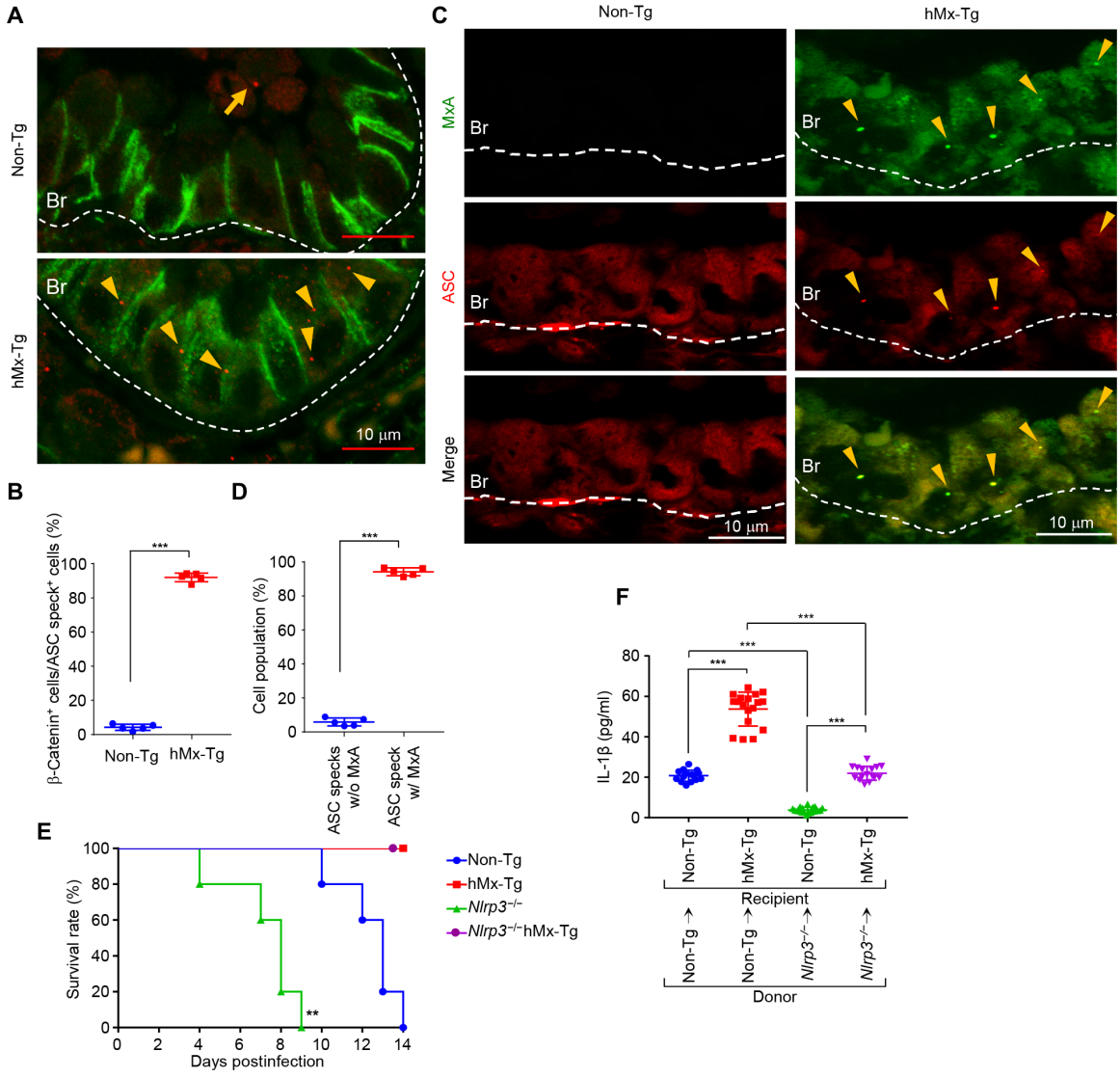

Fig. 7. MxA is required for inflammasome activation in respiratory epithelium in vivo. (**A** to **D**) At day 3 after infection with IAV, lung tissue sections of non-Tg and hMx-Tg mice were subjected to immunohistochemical analysis with either anti–β-catenin (green) and anti-ASC (red) antibodies (A and B) or anti-MxA (green) and anti-ASC (red) antibodies (C and D). ASC specks in epithelial cells (arrowheads) and in immune cells (arrow) are indicated. Br, bronchioles. The number of β-catenin–positive cells among ASC speck–positive cells (B) and the number of cells containing colocalization of ASC speck and MxA in hMx-Tg mice were counted (D). ***$P < 0.001$, two-tailed Student's *t* test. (**E**) Survival rate of non-Tg, *Nlrp3*$^{-/-}$, hMx-Tg, and *Nlrp3*$^{-/-}$hMx-Tg mice infected with 1000 PFU of IAV. **$P < 0.01$ (*Nlrp3*$^{-/-}$ versus *Nlrp3*$^{-/-}$hMx-Tg), log-rank test (Mantel-Cox), $n = 5$ mice per group. (**F**) Bone marrow cells prepared from non-Tg or *Nlrp3*$^{-/-}$ mice were transplanted to indicated recipient mice. At day 3 after infection, secreted IL-1β in BALF was examined by ELISA ($n = 15$ to 19 mice per group). The combined results from two independent experiments are shown. Each symbol represents one mouse. ***$P < 0.001$, two-tailed Student's *t* test. Data are representative of three independent experiments (A and C).

These findings indicate that MxA is required for inflammasome activation in the respiratory epithelium upon IAV infection.

MxA inflammasome restricts the host range of IAVs

Seasonal IAVs, but not avian IAVs, partially escape from restriction by MxA through adaptive mutations in NP viral protein (*22*, *24*, *25*). To elucidate whether the MxA inflammasome determines the host range of IAV, we generated reassortant viruses harboring the *NP* segment from A/Thailand/KAN-1/04 (H5N1; KAN-1), mouse-adapted A/Seal/Mass/1/80 (H7N7; SC35M), A/Hamburg/4/2009 (pH1N1), or A/Brevig Mission/1/1918 (H1N1; 1918) on the A/Puerto Rico/8/34 (H1N1 lab strain; PR8) backbone. KAN-1 and SC35M viruses are mammalian-adapted avian IAVs expected to show inefficient human-to-human transmission. pH1N1, 1918, and PR8 viruses are seasonal IAVs naturally circulating in humans. The *NP* genes of these viruses are more than 93% identical in their amino acid sequences. Although the expression level of NP was comparable between the reassortant viruses, the amount of secreted IL-1β from the H5N1 or the H7N7 reassortant virus-infected PL16T cells was increased by more than threefold compared with pH1N1, 1918, and PR8 at 36 hours after infection (Fig. 8, A and B). Similar results were obtained for cells transfected with NP variants from H5N1, H7N7, or seasonal IAV strains followed by IFN-β treatment (fig. S12). The number of infiltrating granulocytes in BALF obtained from the H5N1 or the

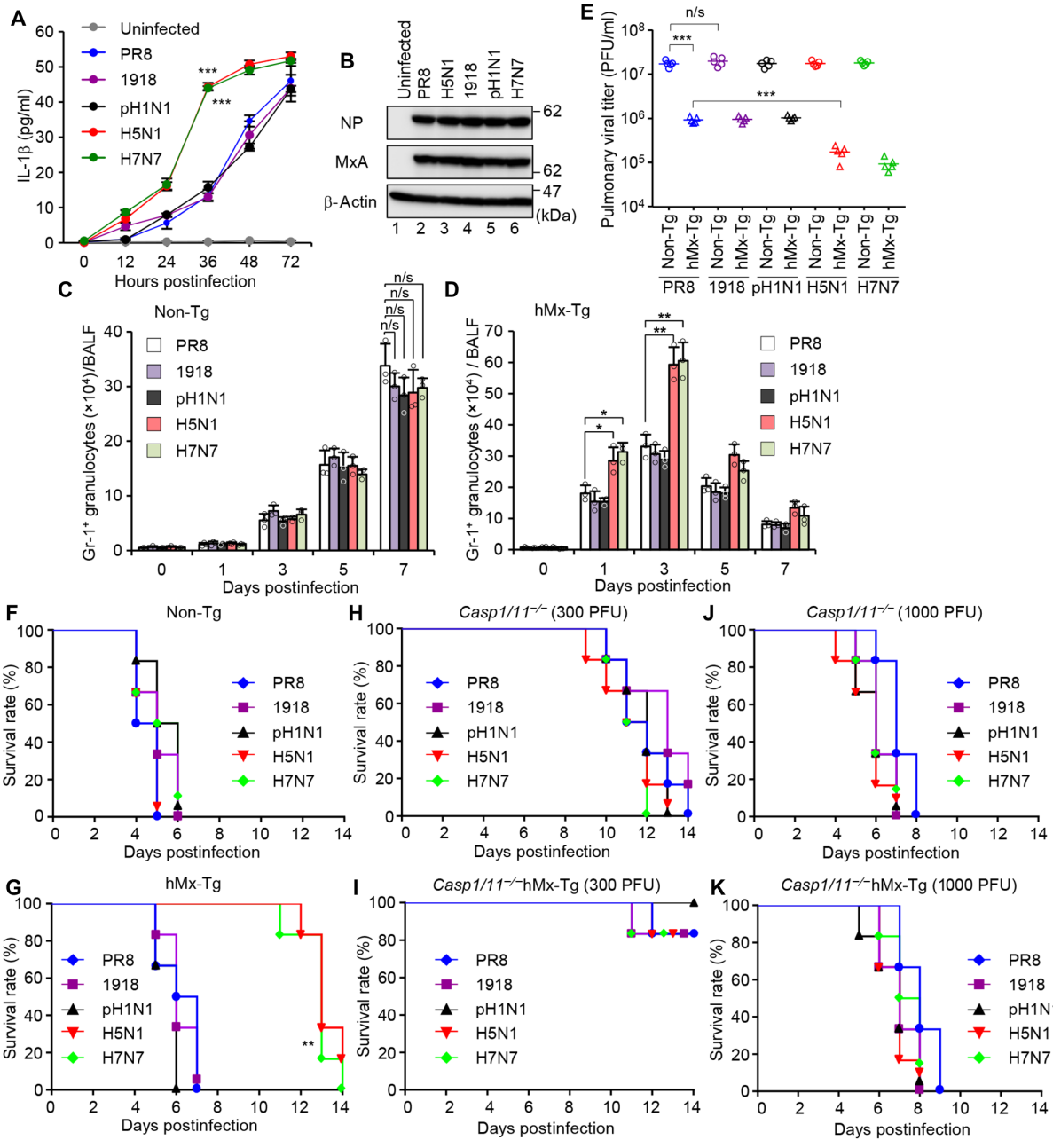

Fig. 8. MxA inflammasome restricts the host range of IAVs. (**A** and **B**) PL16T cells were infected with either PR8 or PR8-based reassortant viruses harboring *NP* gene from 1918, pH1N1, H5N1, or H7N7 strain at MOI of 10. The level of secreted IL-1β (means ± SD from three independent experiments) (A) and the expression level of NP and MxA at 36 hours after infection (B) were examined. ***$P < 0.001$ (H5N1 versus PR8 and H7N7 versus PR8), two-tailed Student's *t* test. Data are representative of three independent experiments (B). (**C** to **E**) Non-Tg and hMx-Tg mice were infected with 3000 PFU of indicated reassortant viruses. The number of Gr-1$^+$ granulocytes in BALF of non-Tg (C) and hMx-Tg (D) mice infected with indicated IAVs was examined by FACS. The pulmonary viral titer at day 5 after infection was examined by plaque assays (E) ($n = 5$ mice per group). *$P < 0.05$, **$P < 0.01$, and ***$P < 0.001$, two-tailed Student's *t* test. Each symbol represents one mouse. (**F** and **G**) Non-Tg (F) and hMx-Tg (G) mice were infected with 10,000 PFU of the indicated IAVs. **$P < 0.01$ (H5N1 versus PR8 and H7N7 versus PR8), log-rank test (Mantel-Cox), $n = 6$ mice per group. The combined results from two independent experiments are shown. (**H** to **K**) Survival rate of *Casp1/11*$^{-/-}$ (H and J) and *Casp1/11*$^{-/-}$hMx-Tg mice (I and K) infected with 300 PFU (H and I) or 1000 PFU (J and K) of the indicated IAVs ($n = 6$ mice per group).

H7N7 reassortant-infected hMx-Tg mice was increased about two-fold compared with those of pH1N1, 1918, and PR8 at day 3 after infection, but no apparent difference was observed in the proinflammatory response between non-Tg mice infected with these reassortant viruses (Fig. 8, C and D). Pulmonary viral titers and survival of non-Tg mice were not changed by the reassortment of *NP* genes between the PR8, H5N1, H7N7, pH1N1, and 1918 strains (Fig. 8, E and F). In contrast, hMx-Tg mice infected with 10,000 plaque-forming units (PFU) of either the H5N1 or the H7N7 reassortant viruses revealed better survival compared with pH1N1, 1918, and

PR8 (Fig. 8G). No such differences between virus strains were observed in *Casp1/11*$^{-/-}$ mice. *Casp1/11*$^{-/-}$hMxTg mice survived infection with 300 PFU of the various reassortant viruses (Fig. 8, H and I), whereas non-Tg *Casp1/11*$^{-/-}$ mice became ill. When the virus challenge dose was enhanced to 1000 PFU (Fig. 8, J and K), all *Casp1/11*$^{-/-}$ mice succumbed to the infection irrespective of whether the MxA transgene was present, suggesting that MxA protects from infections with H5N1 and H7N7 avian IAVs in a *Casp1/11*-dependent manner.

DISCUSSION

MxA is a virus restriction factor known to inhibit IAV replication by interacting with components of viral RNPs, thereby disturbing the nuclear import of viral RNPs (*10*, *17*, *22*). We demonstrated here that MxA plays an additional role in innate antiviral immunity. MxA serves as inflammasome sensor molecule in respiratory epithelial cells and promotes tissue inflammation by sensing the NP of IAV.

We found that IAV infection induced MxA expression in respiratory epithelial cells but not in macrophages (fig. S7). Thus, inflammasome formation in macrophages was not dependent on MxA but rather dependent on NLRP3 (Fig. 2). It is well known that macrophages can express MxA after type I IFN treatment (*45*). We currently do not understand why respiratory epithelial cells differ from macrophages in their abilities to induce MxA expression upon IAV infection. It is possible that the IAV-encoded nonstructural protein 1 (NS1) suppresses type I IFN synthesis more strongly in macrophages than in respiratory epithelial cells. Alternatively, NS1 might repress the production of type I IFN but not type III IFN, which is known to selectively act on epithelial cells (*46*).

Our finding that MxA serves as an inflammasome sensor in the respiratory epithelium is unexpected considering that MxA does not have a PYD domain, which mediates the interaction between ASC and conventional inflammasome sensors such as NLRP3, NLRP1, or AIM2 (*5*). We found that the GTPase domain of MxA was responsible for the physical contact with the PYD domain of ASC (Fig. 1, D and E). Complex formation of MxA and ASC does not seem to require any additional mammalian factors because it could be biochemically reconstructed using recombinant proteins purified from bacterial expression systems. Of note, although binding of ASC is mediated by monomeric MxA, oligomerization of MxA is responsible for inflammasome activation. We previously reported that epithelial cell lines isolated from malignant lung tumors could not activate inflammasomes upon IAV infection even after type I IFN treatment (*8*), indicating that induced expression of MxA is not sufficient to oligomerize ASC. This suggests that MxA requires other regulatory mechanisms for inflammasome activation, which may be impaired during development of malignant tumors. To elucidate the mechanism of MxA inflammasome formation, identification of regulatory factors and additional structural studies, including fine-mapping the interaction surface between MxA and ASC, will be required. Except for human primary epithelial cells, only the nonmalignant immortalized cell line, PL16T cells, can be used to activate the MxA inflammasome. One of the experimental limitations in the MxA inflammasome is that PL16T cells are difficult to maintain because of slow growth.

The expression of MxA is regulated by type I and III IFNs, which are secreted from infected cells and induce IFN-stimulated genes in an autocrine/paracrine-dependent manner (*10*). Thus, MxA is expressed not only in infected cells but also in uninfected cells away from the infected cells by the paracrine mechanism. We found that the direct inhibition of viral replication by MxA was observed only in cells expressing MxA before infection but not after infection (Fig. 5C). Thus, it is possible that the MxA-mediated direct inhibition is crucial for the antiviral defense in distal regions away from initial infection sites through the MxA expression before the spread of progeny viruses.

A cluster of a few amino acid residues, which have been shown to be responsible for MxA sensitivity, was identified in the surface-exposed domain of NP (*24*). These amino acid residues are highly conserved in seasonal IAVs but not in avian IAVs isolated from human cases, suggesting that the escape mutations from MxA restriction are crucial for seasonal IAV (*22*, *24*, *25*). MxA restricts avian IAV strains more strongly than seasonal IAV strains through the classical and the newly discovered antiviral pathways (Fig. 8), indicating that MxA is one of the host range determinants of avian IAVs. This also implies that viral target recognition by MxA must be quite similar between these pathways. Further, MxA is known to target the nucleocapsid protein of other viruses, including thogotovirus, vesicular stomatitis virus, human parainfluenza virus, and bunyaviruses. It will also be interesting to reveal how MxA recognizes a common structural pattern shared among these viruses.

MATERIALS AND METHODS

TR-FRET assay

His-MxA (residues 1 to 662), His-MxA-GTPase [residues 38 to 366-$(GS)_5$–622 to 662], and His-MxA-stalk (residues 367 to 621) were cloned into pSKB2 and were expressed in *Escherichia coli* strain BL21(DE3) pLysS. MBP-ASC (residues 1 to 195), MBP-ASC-PYD (residues 1 to 106), and MBP-ASC-CARD (residues 107 to 195) were cloned into pMAL with a peptide sequence (GLNDIFEAQKIEWHE), which is biotinylated by biotin ligase BirA, at the C terminus of each protein. The MBP-ASC proteins were expressed in *E. coli* strain BL21(DE3) expressing BirA in the presence of 50 μM biotin. The recombinant proteins were purified according to the manufacturer's protocol. After further purification on a MonoQ column (GE Healthcare) with a linear gradient of 50 to 500 mM NaCl, purified proteins were applied to a HiTrap desalting column (GE Healthcare) in a buffer containing 50 mM Hepes-NaOH (pH 7.9), 150 mM NaCl, 3 mM $MgCl_2$, and 10% glycerol. The purified recombinant proteins were incubated at 30°C for 1 hour in a buffer containing 20 mM Hepes-NaOH (pH 7.9), 50 mM NaCl, 3 mM $MgCl_2$, and 0.0004% bovine serum albumin, and the interaction was quantified using TR-FRET assays with streptavidin-d2 and anti–6HIS-Tb cryptate (Cisbio). The ratio of the emission wavelengths specific for the acceptor fluorophore d2 (665 nm) and the donor fluorophore Tb (620 nm) was converted to ΔF [ΔF (%) = 100 × (sample ratio – background ratio)/(background ratio)] to normalize experiments.

ASC oligomerization assay

Cells were permeabilized with phosphate-buffered saline (PBS) containing 0.5% Triton X-100 and then cross-linked at room temperature for 30 min by adding 2 mM bis(sulfosuccinimidyl) suberate (BS^3) (Thermo Fisher Scientific, cat. no. 21586). After cell lysis in an SDS sample buffer, the lysates were analyzed by 12.5% SDS–polyacrylamide gel electrophoresis (PAGE), followed by Western blotting assays with rabbit anti-ASC antibody.

Mice

Human MxA-transgenic mice (hMx-Tg) on a C57BL/6 background were previously described (*21*). *Nlrp3*$^{-/-}$ and *Casp1/11*$^{-/-}$ mice were purchased from the Jackson Laboratory. *Casp1/11*$^{-/-}$ or *Nlrp3*$^{-/-}$ mice were crossed with hMx-Tg mice to generate homozygous knockouts. All in vivo experiments were carried out according to the Guideline for Proper Conduct of Animal Experiments, Science Council of Japan. The protocols for the mouse experiments were approved by the Animal Care and Use Committee of the University of Tsukuba.

Influenza virus and *S. typhimurium* infection of mice

Eight-week-old mice were anesthetized by intraperitoneal injection of pentobarbital sodium and then infected with 300 (for body weight loss), 1000 (for body weight loss), 3000 (for histological analysis, cytokine production, and viral titer), or 10,000 (for body weight loss) PFU of IAV in 50 μl of PBS via intranasal administration. For the *S. typhimurium* infection, 8-week-old mice were kept without food for 12 hours and then infected with 1×10^5, 1×10^6, or 1×10^7 colony-forming units (CFU) of *S. typhimurium* in 100 μl of PBS using an oral zonde needle.

Bone marrow transplantation

Recipient mice were irradiated (2 × 4.5 gray) using an MBR-1520R irradiator (Hitachi). At 24 hours after irradiation, 5×10^5 of bone marrow cells collected from donor mice were injected into the recipient mice from the tail vein. At 8 weeks after bone marrow transplantation, the chimeric mice were infected with 3000 PFU of IAV.

Flow cytometry

Cells were collected from BALF and resuspended in a buffer containing 154 mM NH_4Cl, 10 mM $KHCO_3$, and 0.1 mM EDTA for red blood cell lysis for 5 min. After washing with PBS containing 2% fetal bovine serum, cells were stained with either anti–Gr-1 (cat. no. 108412; BioLegend) or anti–immunoglobulin G2a (IgG2a) (BioLegend, cat. no. 407109) antibodies for 30 min on ice. To confirm the efficiency of bone marrow transplantation, cells were collected from the bone marrow of the chimeric mice. After fixing with 3% paraformaldehyde, cells were permeabilized and incubated with allophycocyanin (APC)–conjugated anti–Mac-1 (CD11b) (BioLegend, cat. no. 101211) and mouse anti-NLRP3 antibodies for 1 hour. After washing with PBS containing 0.2% Tween 20, cells were incubated with Alexa Fluor 488–conjugated anti-mouse IgG antibody (Invitrogen, cat. no. A11029) for 30 min. Flow cytometry analysis was performed using a Guava easyCyte flow cytometer (Merck Millipore).

Statistical analysis

Statistical significance was tested using a two-tailed Student's *t* test. n/s, not significant. ***$P < 0.001$, **$P < 0.01$, and *$P < 0.05$. Survival curves were analyzed using the log-rank (Mantel-Cox) test.

SUPPLEMENTARY MATERIALS

immunology.sciencemag.org/cgi/content/full/4/40/eaau4643/DC1
Materials and Methods
Fig. S1. Schematic diagram of high-content screening with lentiviral shRNA library.
Fig. S2. Expression level of target genes in shRNA-treated PL16T and THP-1 cells.
Fig. S3. Expression level of NP viral protein in shRNA-treated PL16T and THP-1 cells.
Fig. S4. Purification of recombinant proteins.
Fig. S5. MxA is required for IL-18 secretion from infected PL16T cells upon IAV infection.
Fig. S6. AIM2 and NLRC4 are not required for IL-1β secretion in PL16T cells upon IAV infection.
Fig. S7. Expression level of MxA, NLRP3, and caspase-1 in respiratory epithelial cells and macrophages.
Fig. S8. Expression level of NP viral protein in MxA KD PL16T cells exogenously expressing NLRP3.
Fig. S9. Expression level of viral proteins in transfected PL16T cells.
Fig. S10. ASC oligomerization and proteolytic activation of caspase-1 in IAV-infected NHBE cells.
Fig. S11. Efficiency of bone marrow transplantation.
Fig. S12. Inflammasome activation by H5N1 or H7N7 NP transfection.
Data file S1. Raw data (Excel).
Reference (*47*)

View/request a protocol for this paper from *Bio-protocol*.

REFERENCES AND NOTES

1. T. Ichinohe, H. K. Lee, Y. Ogura, R. Flavell, A. Iwasaki, Inflammasome recognition of influenza virus is essential for adaptive immune responses. *J. Exp. Med.* **206**, 79–87 (2009).
2. T. D. Kanneganti, M. Body-Malapel, A. Amer, J. H. Park, J. Whitfield, L. Franchi, Z. F. Taraporewala, D. Miller, J. T. Patton, N. Inohara, G. Núñez, Critical role for Cryopyrin/Nalp3 in activation of caspase-1 in response to viral infection and double-stranded RNA. *J. Biol. Chem.* **281**, 36560–36568 (2006).
3. P. G. Thomas, P. Dash, J. R. Aldridge Jr., A. H. Ellebedy, C. Reynolds, A. J. Funk, W. J. Martin, M. Lamkanfi, R. J. Webby, K. L. Boyd, P. C. Doherty, T.-D. Kanneganti, The intracellular sensor NLRP3 mediates key innate and healing responses to influenza A virus via the regulation of caspase-1. *Immunity* **30**, 566–575 (2009).
4. I. C. Allen, M. A. Scull, C. B. Moore, E. K. Holl, E. McElvania-TeKippe, D. J. Taxman, E. H. Guthrie, R. J. Pickles, J. P.-Y. Ting, The NLRP3 inflammasome mediates in vivo innate immunity to influenza A virus through recognition of viral RNA. *Immunity* **30**, 556–565 (2009).
5. D. E. Place, T.-D. Kanneganti, Recent advances in inflammasome biology. *Curr. Opin. Immunol.* **50**, 32–38 (2018).
6. T. Ichinohe, I. K. Pang, A. Iwasaki, Influenza virus activates inflammasomes via its intracellular M2 ion channel. *Nat. Immunol.* **11**, 404–410 (2010).
7. J. A. Whitsett, T. Alenghat, Respiratory epithelial cells orchestrate pulmonary innate immunity. *Nat. Immunol* **16**, 27–35 (2015).
8. S. Lee, M. Hirohama, M. Noguchi, K. Nagata, A. Kawaguchi, Influenza A virus infection triggers pyroptosis and apoptosis of respiratory epithelial cells through type I Interferon signaling pathway in a mutually exclusive manner. *J. Virol.* **92**, e00396-18 (2018).
9. O. Haller, G. Kochs, Human MxA protein: An interferon-induced dynamin-like GTPase with broad antiviral activity. *J. Interferon Cytokine Res.* **31**, 79–87 (2011).
10. O. Haller, P. Staeheli, M. Schwemmle, G. Kochs, Mx GTPases: Dynamin-like antiviral machines of innate immunity. *Trends Microbiol.* **23**, 154–163 (2015).
11. G. Kochs, M. Haener, U. Aebi, O. Haller, Self-assembly of human MxA GTPase into highly ordered dynamin-like oligomers. *J. Biol. Chem.* **277**, 14172–14176 (2002).
12. M. A. Accola, B. Huang, A. Al Masri, M. A. McNiven, The antiviral dynamin family member, MxA, tubulates lipids and localizes to the smooth endoplasmic reticulum. *J. Biol. Chem.* **277**, 21829–21835 (2002).
13. S. Gao, A. von der Malsburg, S. Paeschke, J. Behlke, O. Haller, G. Kochs, O. Daumke, Structural basis of oligomerization in the stalk region of dynamin-like MxA. *Nature* **465**, 502–506 (2010).
14. S. Gao, A. von der Malsburg, A. Dick, K. Faelber, G. F. Schröder, O. Haller, G. Kochs, O. Daumke, Structure of myxovirus resistance protein a reveals intra- and intermolecular domain interactions required for the antiviral function. *Immunity* **35**, 514–525 (2011).
15. J. Pavlovic, T. Zürcher, O. Haller, P. Staeheli, Resistance to influenza virus and vesicular stomatitis virus conferred by expression of human MxA protein. *J. Virol.* **64**, 3370–3375 (1990).
16. J. Pavlovic, O. Haller, P. Staeheli, Human and mouse Mx proteins inhibit different steps of the influenza virus multiplication cycle. *J. Virol.* **66**, 2564–2569 (1992).
17. H. Xiao, M. J. Killip, P. Staeheli, R. E. Randall, D. Jackson, The human interferon-induced MxA protein inhibits early stages of influenza A virus infection by retaining the incoming viral genome in the cytoplasm. *J. Virol.* **87**, 13053–13058 (2013).
18. G. Kochs, O. Haller, Interferon-induced human MxA GTPase blocks nuclear import of Thogoto virus nucleocapsids. *Proc. Natl. Acad. Sci. U.S.A.* **96**, 2082–2086 (1999).
19. O. Haller, S. Gao, A. von der Malsburg, O. Daumke, G. Kochs, Dynamin-like MxA GTPase: Structural insights into oligomerization and implications for antiviral activity. *J. Biol. Chem.* **285**, 28419–28424 (2010).
20. D. Dornfeld, P. P. Petric, E. Hassan, R. Zell, M. Schwemmle, Eurasian Avian-like swine influenza A viruses escape human MxA restriction through distinct mutations in their nucleoprotein. *J. Virol.* **93**, e00997-18 (2019).
21. C. M. Deeg, E. Hassan, P. Mutz, L. Rheinemann, V. Götz, L. Magar, M. Schilling, C. Kallfass, C. Nurnberger, S. Soubies, G. Kochs, O. Haller, M. Schwemmle, P. Staeheli, In vivo evasion of MxA by Avian influenza viruses requires human signature in the viral nucleoprotein. *J. Exp. Med.* **214**, 1239–1248 (2017).

22. V. Götz, L. Magar, D. Dornfeld, S. Giese, A. Pohlmann, D. Höper, B. W. Kong, D. A. Jans, M. Beer, O. Haller, M. Schwemmle, Influenza A viruses escape from MxA restriction at the expense of efficient nuclear vRNP import. *Sci. Rep.* **6**, 23138 (2016).
23. D. Riegger, R. Hai, D. Dornfeld, B. Mänz, V. Leyva-Grado, M. T. Sanchez-Aparicio, R. A. Albrecht, P. Palese, O. Haller, M. Schwemmle, A. Garcia-Sastre, G. Kochs, M. Schmolke, The nucleoprotein of newly emerged H7N9 influenza A virus harbors a unique motif conferring resistance to antiviral human MxA. *J. Virol.* **89**, 2241–2252 (2015).
24. B. Mänz, D. Dornfeld, V. Götz, R. Zell, P. Zimmermann, O. Haller, G. Kochs, M. Schwemmle, Pandemic influenza A viruses escape from restriction by human MxA through adaptive mutations in the nucleoprotein. *PLOS Pathog.* **9**, e1003279 (2013).
25. P. Zimmermann, B. Mänz, O. Haller, M. Schwemmle, G. Kochs, The viral nucleoprotein determines Mx sensitivity of influenza A viruses. *J. Virol.* **85**, 8133–8140 (2011).
26. R. Zhou, A. S. Yazdi, P. Menu, J. Tschopp, A role for mitochondria in NLRP3 inflammasome activation. *Nature* **469**, 221–225 (2011).
27. V. Hornung, A. Ablasser, M. Charrel-Dennis, F. Bauernfeind, G. Horvath, D. R. Caffrey, E. Latz, K. A. Fitzgerald, AIM2 recognizes cytosolic dsDNA and forms a caspase-1-activating inflammasome with ASC. *Nature* **458**, 514–518 (2009).
28. Y. Zhao, J. Yang, J. Shi, Y.-N. Gong, Q. Lu, H. Xu, L. Liu, F. Shao, The NLRC4 inflammasome receptors for bacterial flagellin and type III secretion apparatus. *Nature* **477**, 596–600 (2011).
29. G. Guarda, M. Zenger, A. S. Yazdi, K. Schroder, I. Ferrero, P. Menu, A. Tardivel, C. Mattmann, J. Tschopp, Differential expression of NLRP3 among hematopoietic cells. *J. Immunol.* **186**, 2529–2534 (2011).
30. K. Turan, M. Mibayashi, K. Sugiyama, S. Saito, A. Numajiri, K. Nagata, Nuclear MxA proteins form a complex with influenza virus NP and inhibit the transcription of the engineered influenza virus genome. *Nucleic Acids Res.* **32**, 643–652 (2004).
31. Y. He, M. Y. Zeng, D. Yang, B. Motro, G. Núñez, NEK7 is an essential mediator of NLRP3 activation downstream of potassium efflux. *Nature* **530**, 354–357 (2016).
32. C. Di Paolo, H. P. Hefti, M. Meli, H. Landis, J. Pavlovic, Intramolecular backfolding of the carboxyl-terminal end of MxA protein is a prerequisite for its oligomerization. *J. Biol. Chem.* **274**, 32071–32078 (1999).
33. A. Ponten, C. Sick, M. Weeber, O. Haller, G. Kochs, Dominant-negative mutants of human MxA protein: Domains in the carboxy-terminal moiety are important for oligomerization and antiviral activity. *J. Virol.* **71**, 2591–2599 (1997).
34. A. von der Malsburg, I. Abutbul-Ionita, O. Haller, G. Kochs, D. Danino, Stalk domain of the dynamin-like MxA GTPase protein mediates membrane binding and liposome tubulation via the unstructured L4 loop. *J. Biol. Chem.* **286**, 37858–37865 (2011).
35. J. Verhelst, P. Hulpiau, X. Saelens, Mx proteins: Antiviral gatekeepers that restrain the uninvited. *Microbiol. Mol. Biol. Rev.* **77**, 551–566 (2013).
36. O. Haller, S. Stertz, G. Kochs, The Mx GTPase family of interferon-induced antiviral proteins. *Microbes Infect.* **9**, 1636–1643 (2007).
37. D. Grimm, P. Staeheli, M. Hufbauer, I. Koerner, L. Martínez-Sobrido, A. Solórzano, A. García-Sastre, O. Haller, G. Kochs, Replication fitness determines high virulence of influenza A virus in mice carrying functional Mx1 resistance gene. *Proc. Natl. Acad. Sci. U.S.A.* **104**, 6806–6811 (2007).
38. T. M. Tumpey, K. J. Szretter, N. Van Hoeven, J. M. Katz, G. Kochs, O. Haller, A. García-Sastre, P. Staeheli, The Mx1 gene protects mice against the pandemic 1918 and highly lethal human H5N1 influenza viruses. *J. Virol.* **81**, 10818–10821 (2007).
39. O. Haller, M. Frese, D. Rost, P. A. Nuttall, G. Kochs, Tick-borne thogoto virus infection in mice is inhibited by the orthomyxovirus resistance gene product Mx1. *J. Virol.* **69**, 2596–2601 (1995).
40. J. Pavlovic, H. A. Arzet, H. P. Hefti, M. Frese, D. Rost, B. Ernst, E. Kolb, P. Staeheli, O. Haller, Enhanced virus resistance of transgenic mice expressing the human MxA protein. *J. Virol.* **69**, 4506–4510 (1995).
41. G. Kochs, C. Janzen, H. Hohenberg, O. Haller, Antivirally active MxA protein sequesters La Crosse virus nucleocapsid protein into perinuclear complexes. *Proc. Natl. Acad. Sci. U.S.A.* **99**, 3153–3158 (2002).
42. M. Palm, M. M. Garigliany, F. Cornet, D. Desmecht, Interferon-induced Sus scrofa Mx1 blocks endocytic traffic of incoming influenza A virus particles. *Vet. Res.* **41**, 29 (2010).
43. P. Staeheli, R. Grob, E. Meier, J. G. Sutcliffe, O. Haller, Influenza virus-susceptible mice carry Mx genes with a large deletion or a nonsense mutation. *Mol. Cell. Biol.* **8**, 4518–4523 (1988).
44. L. Franchi, A. Amer, M. Body-Malapel, T.-D. Kanneganti, N. Özören, R. Jagirdar, N. Inohara, P. Vandenabeele, J. Bertin, A. Coyle, E. P. Grant, G. Núñez, Cytosolic flagellin requires Ipaf for activation of caspase-1 and interleukin 1beta in salmonella-infected macrophages. *Nat. Immunol.* **7**, 576–582 (2006).
45. T. Ronni, S. Matikainen, A. Lehtonen, J. Palvimo, J. Dellis, F. Van Eylen, J. F. Goetschy, M. Horisberger, J. Content, I. Julkunen, The proximal interferon-stimulated response elements are essential for interferon responsiveness: A promoter analysis of the antiviral MxA gene. *J. Interferon Cytokine Res.* **18**, 773–781 (1998).
46. C. Sommereyns, S. Paul, P. Staeheli, T. Michiels, IFN-lambda (IFN-λ) is expressed in a tissue-dependent fashion and primarily acts on epithelial cells in vivo. *PLOS Pathog.* **4**, e1000017 (2008).
47. A. Kawaguchi, K. Nagata, De novo replication of the influenza virus RNA genome is regulated by DNA replicative helicase, MCM. *EMBO J.* **26**, 4566–4575 (2007).

Acknowledgments: We thank T. Ichinohe (The University of Tokyo) for the gifts of pCA7-ASC and pCA7-NLRP3 plasmids and M. Yamashita and J. H. Choi (University of Tsukuba) for technical support. We also thank F. Miyamasu (Medical English Communications Center, University of Tsukuba) for critical review of the manuscript. **Funding:** This research was supported, in part, by grant-in-aids from the Ministry of Education, Culture, Sports, Science, and Technology of Japan (16H05192 and 19H03475 to A.K. and 24115002 to K.N.); from AMED (JP18fk0108076 to A.K.); from NOMURA Microbial Community Control Project in ERATO of the Japan Science and Technology Agency (to A.K.); and from the Deutsche Forschungsgemeinschaft (SFB 1160 to P.S. and M.S.). **Author contributions:** S.L. and A.K. conceived and designed the experiments. S.L., M.H., A.I., Y.F., P.P.P., and A.K. performed the experiments including statistical analysis. S.L., A.I., M.N., P.S., M.S., K.N., and A.K. analyzed the data. S.L., A.I., P.S., M.S., K.N., and A.K. contributed reagents/materials/analysis tools. S.L., P.S., K.N., and A.K. wrote the manuscript. **Competing interests:** The authors declare that they have no competing financial interests. **Data and materials availability:** All data needed to evaluate the conclusions in the paper are present in the paper or the Supplementary Materials. Further information and requests for resources and reagents should be directed and will be fulfilled by the corresponding author, A.K. (ats-kawaguchi@md.tsukuba.ac.jp).

Submitted 13 June 2018
Resubmitted 21 June 2019
Accepted 19 September 2019
Published 25 October 2019
10.1126/sciimmunol.aau4643

Citation: S. Lee, A. Ishitsuka, M. Noguchi, M. Hirohama, Y. Fujiyasu, P. P. Petric, M. Schwemmle, P. Staeheli, K. Nagata, A. Kawaguchi, Influenza restriction factor MxA functions as inflammasome sensor in the respiratory epithelium. *Sci. Immunol.* **4**, eaau4643 (2019).

Science Immunology

Influenza restriction factor MxA functions as inflammasome sensor in the respiratory epithelium

SangJoon Lee, Akari Ishitsuka, Masayuki Noguchi, Mikako Hirohama, Yuji Fujiyasu, Philipp P. Petric, Martin Schwemmle, Peter Staeheli, Kyosuke Nagata and Atsushi Kawaguchi

Sci. Immunol. **4**, eaau4643.
DOI: 10.1126/sciimmunol.aau4643

Influenza and the inflammasome

Influenza A virus (IAV) infection triggers multiple inflammatory responses in the respiratory mucosa, including the release of proinflammatory cytokines like IL-1 β through inflammasome activation. The mechanism by which IAV activates inflammasomes has been unclear, but Lee *et al.* have now identified human myxoma resistance protein 1 (MxA) as an inflammasome sensor protein in human respiratory epithelial cells. MxA recognizes IAV nucleoprotein and interacts with ASC to trigger ASC oligomerization, inflammasome formation, and IL-1β secretion. In transgenic mice expressing human MxA, IAV infection was curbed due to rapid IL-1 β secretion in the respiratory epithelium. These findings indicate that MxA can function as an inflammasome sensor during respiratory infection with IAV.